Role of Fibrinogen Conformation in Platelet Activation

A. Chiumiento, S. Lamponi, and R. Barbucci*

CRISMA and Department of Chemical and Biosystem Sciences and Technologies, University of Siena, Via A. Moro n. 2, Siena 53100, Italy

Received July 10, 2006; Revised Manuscript Received October 4, 2006

Platelet adhesion and activation induced by fibrinogen (Fbg) coating on polysaccharide layers of hyaluronic acid (Hyal) and its sulfated derivative (HyalS) were analyzed. Hyal or HyalS was coated and grafted on the glass substrate using a photolithographic method. The Fbg coating was achieved by two different routes: the immobilization of Fbg by means of covalent bond to the polysaccharide layers and the mere adsorption of Fbg to Hyal and HyalS surfaces. Platelet adhesion and activation to the surfaces were evaluated using, respectively, scanning electron microscopy (SEM) and quantifying the release of Platelet Factor 4 by ELISA. The method used for the coating of the surfaces with the Fbg influenced the platelet response. In fact, platelet adhesion and activation took place on surfaces covered by bound Fbg but not on those containing adsorbed Fbg. To explain this difference, the molecular mechanism involved in the Fbg−platelet interaction was investigated blocking platelet membrane receptors by monoclonal antibodies. Because the interaction between Fbg and the GPIIb/IIIa platelet membrane receptor was the only molecular pathway involved, Fbg conformation after the interaction (adsorption or binding) with the Hyal and the HyalS chains and the role of serum proteins adsorbed on the Fbg containing surfaces were accurately analyzed. Both adsorbed and bound Fbg prevented the adsorption of further serum proteins; consequently, a direct interaction between Fbg and platelets was supposed and the different platelet behavior was ascribed to the different conformational changes that occurred after the adsorption and the chemical binding of the Fbg to the Hyal and HyalS surfaces.

Introduction

The cell response to a biocompatible surface is deeply affected by the spontaneous formation of a protein layer at the interface.[1−4]

This work is aimed at understanding the phenomena occurring when a biomaterial, properly modified by adsorbing or chemically grafting specific molecules for cell-adhesion receptors, is incubated with cells, platelets, or physiological fluids.

Previously, we focused our attention on fibronectin (Fn), an extracellular matrix protein with well-known cell-adhesive properties:[5,6] Fn was adsorbed and chemically bound to hyaluronic acid or its sulfated derivative surfaces;[7] both adsorbed and bound fibronectin enhance adhesion of the human fibroblasts on the polysaccharide surfaces in vitro. In this work, we prepared biologically functional materials, by adsorbing and, alternately, chemically grafting the human fibrinogen to hyaluronic acid (Hyal) and sulfated hyaluronic acid (HyalS) surfaces to evaluate the correlation between adsorbed and immobilized fibrinogen (Fbg) conformation and cell response.

Polysaccharides are composed of hundreds or thousands of monosaccharide units linked by glucosidic bonds. They represent a major class of biological macromolecules that occur throughout nature.

Among polysaccharides, hyaluronan has attracted a great deal of interest in the biomaterials and tissue engineering fields. Hyaluronan is a linear poly anionic polymer with a high molecular weight consisting of alternating *N*-acetyl-D-glucosamine and β-D-glucuronic acid residues linked 1−3 and 1−4, respectively (Figure 1a).[8]

Hyal is highly hydrophilic for the presence of hydroxyl, amide, and carboxyl groups. This natural proteoaminoglycan is one of the major components of synovial fluids; it can be found in the central nervous system and in the cartilage matrix. It represents one of the glycosaminoglycan components of the extracellular matrix (ECM),[9,10] it is produced at the plasma membrane by Hyal synthetase, and it is extruded outside the cell.[11] Its synthesis increases during cell migration,[16] mitosis,[17] and cancer invasion.[12] Moreover, it plays a key role in wound healing during the granulation phase, demonstrating anti-inflammatory effects[13] as well as inhibitory effects on prostaglandin synthesis.[14]

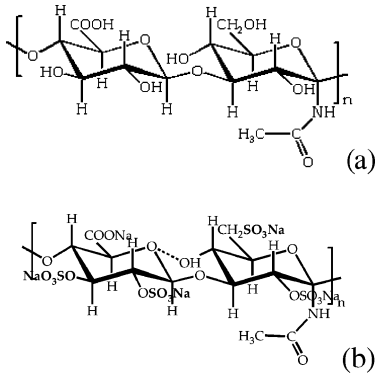

Figure 1. Disaccharide unit of hyaluronic acid (a) and of sulfated hyaluronan sodium salt (b).

Purified hyaluronan has been employed as a structural material thanks to its high molecular weight and capability to form 3D networks. The properties of this macromolecule may be regulated by chemical modifications. Partial esterification of the carboxylic groups reduces the water solubility of the polymer and increases the viscosity. Ethyl and benzyl esters have proven to be excellent membranes or scaffolds for cell growth.[15] By making intra- and/or interchains cross-link, hy-

* To whom correspondence should be addressed. Phone: +390577234382. Fax: +390577234383. E-mail: barbucci@unisi.it.

10.1021/bm060664m CCC: $37.00
Published on Web 12/24/2006

drogels with different controlled chemistry and thus different mechanical and biological properties have been obtained.[16]

One of the most interesting chemical modifications of Hyal structure is the insertion of sulfate groups on the hydroxyl groups of the polysaccharide with the aim to obtain a macromolecule with heparin-like activity.[17]

The antithrombotic action of heparin is well known; it stimulates the neutralization of thrombin and factor Xa by antithrombin.[18] However, because the heparin structure is not characterized by a regular sequence, it becomes difficult to get reproducible results and to understand structure−property relationships.

On the contrary, HyalS has a highly ordered and reproducible chemical composition, and its ability to inactivate thrombin and factor Xa, due to the interaction between the polysaccharide and the serine proteases, increases with the increase of the sulfate groups and of its molecular weight.[19]

All of the materials used in medical devices that are to come in contact with blood promote thrombotic activity to various extents; therefore, the biomaterials surface is commonly modified to reduce/prevent platelet adhesion and activation, which promote the coagulation cascade and the thrombus formation.[20]

Several strategies have been developed to obtain antithrombotic materials, including physicochemical processes (plasma/ion beam modification), polymer grafting (PEG and sulfobetaine), and biological methods (e.g., chitosan grafting).[21−24]

All of these methods attempt to prevent the nonspecific adsorption on the biomaterial surface of proteins that mediate platelet adhesion. Among them, Fbg has great relevance because it tends to adsorb in high quantity on the biomaterial surfaces. Although the importance of Fbg in mediating platelet adhesion on several biocompatible materials[25−27] has been widely recognized, up to date no studies have been conducted on the role of Fbg in the conformation.

The platelet adhesion receptor system is very well defined.[28−30] Most of the receptors belong to the integrin family, and the fibrinogen receptor (GPIIb-IIIa) is the most abundant and active platelet receptor interacting with the Fbg RGD motif contained in its α-chain, as well as the carboxyl-terminus of its γ-chain.[31−36]

In addition, other integrins with primary, but not exclusive, specificity are present on the platelet membrane, such as the GP Ic/IIa ($\alpha_5\beta_1$) and the GP ($\alpha_5\beta_3$) that play an important role in platelet adhesion to the surfaces of the materials interacting with fibronectin, vitronectin, and laminin. The extent of their involvement is strictly dependent on several factors, among which the surface chemical composition,[37] which can deeply affect the protein conformation and "molecular potency".

The "molecular potency" of a protein in the adsorbed or bound form is strictly connected with the conformation and orientation of the protein interacting with the material.

Most of the techniques used for the analysis of protein structures, such as X-ray crystallography and NMR, are able to provide detailed information about protein conformation, but they cannot be successfully used in the surface analysis. Consequently, the "in situ" analysis of protein conformation is commonly performed using a low-resolution spectroscopic method, such as circular dichroism or attenuated total reflection Fourier-transform infrared (ATR-FTIR) spectroscopy.

The latter permits us to get information about the secondary structure of proteins, without establishing the precise three-dimensional location of individual structural elements.[38] Precisely, FTIR extracts information on protein secondary structures from empirical correlations between the frequencies of certain vibrational modes and the types of secondary structures of polypeptide chains such as α-helix, β-sheet, β-turn, and random coil.

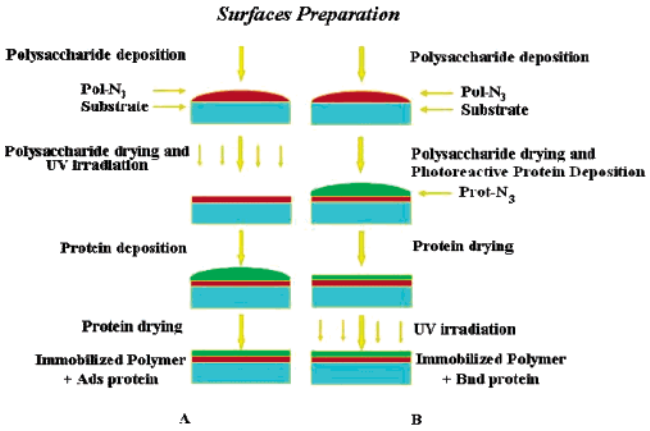

Figure 2. Surfaces preparation.

As a consequence of these site-specific linkage platelets, adhesion as well as platelet activation may take place. The latter phenomenon, called degranulation of platelets, determines a massive release of intracellular-synthesized molecules, such as ADP, serotonin, calcium, platelet factor 4 PF4, etc.

Moreover, to investigate the possible role of other plasma molecules in platelet adhesion and activation on surfaces containing Fbg, the platelet behavior was investigated in the presence of 10% of foetal calf serum [platelets suspended in rich plasma (PRP)].

The presence of plasma proteins adsorbed on our samples was studied utilizing a particular approach for the selective desorption of proteins from the surfaces. It consisted of the sequential use of three different selective eluent solutions, to assess the nature of the forces involved in the interaction on the protein−surface and to discriminate the strength of protein binding to polymer surfaces. The identification of the main serum proteins adsorbed was obtained using SDS-PAGE and Western Blot.

Experimental Section

Materials. The sodium salt of hyaluronan (Hyal-Na, MW 240 000) was supplied by Biophyl S.p.A. (Italy), while its sulfate derivative (HyalS) has been prepared in our laboratories as previously described.[39]

The Dowex 50W 8X resin, the sulfur trioxide complex, 4-azidoaniline hydrochloride, 1-ethyl-3-[3-(dimethyl-amino)propyl] carbodiimide hydrochloride (EDC), and all of the other solvents used for the chemical reactions, as well as foetal calf serum (CFS) and all other reagents, were purchased from Fluka-Sigma-Aldrich Spa (Germany); fibrinogen powder was purchased from Calbiochem Inc.

Methods (see Figure 2). *Preparation of Polysaccharide−Protein Surfaces.* The preparation of polysaccharide−protein surfaces involved three sequential steps: (1) aminosilanization of the glass substrate; (2) synthesis of the photoreactive polysaccharides (Hyal-N_3 or HyalS-N_3) and grafting of the polysaccharides onto the aminosilanized glass; (3a) synthesis of the photoreactive fibrinogen (Fbg-N_3) and its binding onto the polysaccharide surfaces, or (3b) adsorption of the native Fbg on the photoreactive polysaccharides [step 3a excludes 3b and vice versa].

Aminosilanization of the Glass Substrate. To provide superficial binding sites to the polysaccharide chains, as well as to increase the hydrophilicity of the surface, the glass coverslips were aminosilanized as follows:[40] 12 mm diameter glass coverslips were first cleaned using Caro's solution, and then soaked in 0.5 M NaOH solution to remove the excess acid. After that, they were incubated in a 1% solution of 3-aminopropyl-3-aminoethyl-trimethoxysilane in acetic ethanol (pH 5)

Table 1. Sample Abbreviations

sample	
Hyal with bound fibrinogen	Hyal-Fbg_{Bnd}
HyalS with bound fibrinogen	HyalS-Fbg_{Bnd}
Hyal with adsorbed fribrinogen	Hyal-Fbg_{Ads}
HyalS with adsorbed fibrinogen	HyalS-Fbg_{Ads}

for 20 min followed by alternate washing with ethanol and distilled water. The coverslips were then dried using a flow of compressed air.

Synthesis of the Photoreactive Polysaccharides and Their Grafting on the Substrate. The conjugation of Hyal or HyalS with the 4-azidoaniline (photoreactive unit) was obtained as previously reported.[21] Briefly, an established molar ratio (1:2:2) of Hyal-Na or HyalS-Na, 4-azidoaniline hydrochloride, and EDC, respectively, was dissolved in double distilled water. The solution was stirred at 4 °C for 24 h in dark conditions, dialyzed against double distilled water in a dialysis tube with a 12 KDa cutoff, and then freeze-dried. The photoreactive polysaccharides were referred to as Hyal-N_3 or HyalS-N_3, respectively.

Afterward, a 1 mg/mL aqueous solution of the photoreactive polysaccharide (1 mg/mL) was deposited on the pretreated glass substrates and irradiated with a UV source (Helios Italquartz GRE, power 400 W) at a distance of 40 cm for 60 s. The success of the reaction was checked by infrared spectroscopy to identify the presence of the azide group[41] (data not shown).

Synthesis of the Photoreactive Fibrinogen and Its Binding to the Polysaccharide Surfaces. To bind Fbg to Hyal/HyalS film using the photoimmobilization process, it was also necessary to conjugate the Fbg with the 4-azidoaniline molecules. Fibrinogen, the 4-azidoaniline hydrochloride, and the 1-ethyl-3-[3-(dimethyl-amino)propyl] carbodiimide hydrochloride (EDC) were dissolved in PBS pH 7.4 at the established molar ratio of 1:2:2, respectively, and the reaction was conducted for 24 h, at +4 °C, in dark conditions and under constant magnetic stirring. The solution was then dialyzed against a solution of PBS pH 7.4 in a dialysis tube with a cutoff of 12 kDa. In the end, the samples were freeze-dried. The photoreactive Fbg was referred to as Fbg-N_3. The success of the reaction was checked by infrared spectroscopy to identify the presence of the azide group (data not shown).

Afterward, 100 μL of a 0.33 μg/mL solution of Fbg-N_3 was cast onto the photoreactive polysaccharide surfaces and left to dry in dark conditions. Subsequently, the samples were irradiated with a UV lamp (Helios Italquartz 400 W) for 60 s at a distance of 40 cm from the source. The unbound Fbg was removed by washing with PBS and bidistilled water.

Hyal with bound fibrinogen was referred to as Hyal-Fbg_{Bnd} and HyalS with bound fibrinogen as HyalS-Fbg_{Bnd}. See Table 1.

Fibrinogen Adsorption. 100 μL of a PBS (pH 7.4) 0.33 μg/mL solution of Fbg was dropped onto the polysaccharide surfaces and left to adsorb on the layers of Hyal and HyalS for 2 h at 37 °C. All of the surfaces were washed by dipping in double distilled water for 20 min.

The samples obtained with adsorbed fibrinogen (Fbg_{Ads}) were referred to as Hyal-Fbg_{Ads} and HyalS-Fbg_{Ads}. See Table 1.

Biological Analysis. *Platelet Isolation.* Freshly obtained citrated blood from 10 healthy human donors was centrifuged at 150*g* for 15 min at room temperature. After centrifugation, the platelet-rich plasma (PRP) was removed from the basal leukocyte and erythrocyte phase and collected. The final mean concentration of platelets in PRP has been adjusted to 250 000 platelets/μL by dilution with platelet poor plasma (PPP). The PPP was produced by centrifugation of citrated human blood from the same donors at 3000*g* for 10 min at room temperature.

Platelet Adhesion. Scanning electron microscopy (SEM, XL20 Philips, The Netherlands) has been used to characterize platelet adhesion. The analysis has been performed in triplicate for each sample.

Each material was placed at the bottom of a 24 multiwell plate and incubated for 3 h at 37 °C with 1 mL of PRP in static conditions.

Table 2. Classification of Adherent Platelets as a Function of Their Morphology[a]

platelet shape	description of morphology
round (R)	round or disk-shaped morphology and absence of pseudopodia
dendritic (D)	disk-shaped morphology, few pseudopodia, and absence of spreading
spread-dendritic (SD)	with several pseudopodia, some of them flattened onto the material surface and with hyaloplasma expanded among pseudopodia
spreading (S)	with hyaloplasma expanded among pseudopodia
fully spread (FS)	with hyaloplasma completely spread with absence of distinct pseudopodia

[a] Platelet activation: determination of the PF4 release by ELISA test. Commercial enzyme-linked immunosorbent assay (ELISA) platelet activation was used to determine the amount of the released PF4. Activation analysis has been performed in triplicate for each sample.

After incubation, as previously reported,[42] the PRP was removed and the samples were washed with phosphate buffered saline (PBS pH = 7.4) to remove non-adherent platelets.

Next, the adherent platelets were fixed in 2.5% (v/v) glutaraldehyde in 100 mM sodium cacodylate for 30 min, washed in 100 mM cacodylate buffer for 30 s, rinsed with distilled water, and left standing in dehydration solutions (70% v/v, 90% absolute ethanol) for total platelet dehydration. Finally, the samples were desiccated overnight under vacuum and then sputtered with gold.

SEM at 15 kV acceleration voltage was used to observe the total numerical density of the adherent platelets and to describe their characteristic shapes.

Adhered platelet classification has been carried out in accordance with Cooper et al.'s standards,[43] reported in Table 2.

Surfaces have been placed at the bottom of a 24 multiwell plate and incubated for 3 h at 37 °C with 1 mL of PRP in static conditions. After incubation, the PRP was mixed with specific inhibitors and processed according to the instruction manual (AsserachromPF4, Diagnostica Stago, Asniéres, France). Next, the absorbance of the samples was read at 492 nm using a Biotrak II Microplate Reader (Biochrom Ltd., UK). A standard curve, previously obtained using three standard solutions, has been used to extrapolate the PF4 release in each sample from the corresponding absorbance value.

Selective Blocking of GPIIb/IIIa Platelet Membrane Receptor. To understand the mechanism involved in platelet adhesion, the GPIIb/IIIa platelet membrane receptors for Fbg were blocked by monoclonal antibodies in the following way: Nonspecific sites were blocked by suspending trypsinized platelets in 3% bovine serum albumin (BSA) in PBS for 30 min at 37 °C; platelets were centrifuged at 900 rpm for 5 min and suspended in DMEM; 1−0 μL of antibody solution was added to 10^6 cells and incubated at room temperature for 15−30 min; platelets were centrifuged at 900 rpm for 5 min and resuspended in complete DMEM; and 3×10^4 platelets were put in contact with each sample for 24 h at 37 °C in 5% CO_2 humidified atmosphere, and their adhesion was evaluated by scanning electron microscopy (SEM).

The Role of Serum Proteins in the Platelet−Material Interactions. Experiments were performed to investigate the type of serum proteins that adsorb on the polysaccharide surfaces treated with Fbg (Hyal-Fbg_{Ads}, Hyal-Fbg_{Bnd}, HyalS-Fbg_{Ads}, HyalS-Fbg_{Bnd}) when placed in contact with the serum. The presence of proteins was ascertained by SDS-PAGE. Furthermore, the same surfaces were incubated with the platelets.

Evaluation of Adsorbed Serum Proteins by SDS-PAGE. Hyal and HyalS surfaces were incubated for 30 min with serum proteins at 37 °C and then washed with water to remove the loose or non-adsorbed proteins. The supernatants were kept individually in an Eppendorf tube and then freeze-dried.

Afterward, the contribution of electrostatic attraction forces on the protein adsorption was evaluated incubating the surfaces with 500 uL of Laemmli sample buffer [62.5 mM Tris-HCl, pH 6.8; 25% glycerol; 2% SDS 0.01% Bromophenol Blue] four times (20 min time) at room temperature under shaking (using an orbital mixer).

In addition, the classical treatment with SDS was followed by three further elution steps of 20 min each at room temperature with 500 μL of a stronger buffer made of Laemmli buffer, urea 5 M, and 2-mercaptoethanol 5%.[44] In these solutions, the eluting power of SDS was strengthened by the chaotropic action of urea and the reductive action of 2-mercaptoethanol.

At the end, the influence of hydrophobic forces was investigated on fresh samples, previously incubated with serum, using isopropanol/water solution at increasing concentrations (10%, 30%, 50%, 70%) as the eluting agent.

Supernatants were then freeze-dried, and the collected fractions were properly treated to perform the SDS-PAGE. This was done in the following way: Solid lyophilized fraction eluted with water washes and isopropanol/water solutions was resuspended in 15 μL of SDS-PAGE sample buffer [Laemmli buffer and 5% (v/v) of 2-mercaptoethanol], except for the supernatant from the first water wash, which was dissolved in 50 μL.

The fraction eluted with Laemmli buffer was added to a 2-mercaptoethanol, and then all of the fractions were boiled for 3 min and loaded on a 10% acrylamide gel. SDS-PAGE was performed at a 100 kV constant voltage according to Laemmli's method[45] using a Bio-Rad Mini-PROTEAN II system (Bio-Rad, UK). The electrophoresis was also carried out on 15 μL of 0.2% serum in distilled H_2O and of prestained broad range standard by Bio-Rad, used as control. Protein bands were detected by the silver stain procedure[46] using a Silver Stain Plus kit (Bio-Rad SpA) or Sypro Ruby (Bio-Rad SpA).

Instrumental Analysis. *ATR/FTIR Analysis.* Infrared analysis was performed at room temperature using a FT-IR spectrometer Bio-Rad FTS 6000 purged with nitrogen. The ATR spectra of dry samples were recorded with a horizontal (PIKE) ATR accessory equipped with a 45° Ge ATR crystal and a mercurium cadmium telluride (MCT) detector. One hundred and twenty-eight (128) scans at a resolution of 4 cm^{-1} were averaged for each spectrum. Recorded spectra were elaborated by baseline correction (multipoint method) and smoothing (boxcar function; 9 N. of P.) using the software WIN-IR PRO version 2.6.

ATR-FT spectroscopy was used to study the conformational changes of bound or adsorbed Fbg, taking into account the amide I region (1690−1620 cm^{-1}) of the spectrum.

The polysaccharide (Hyal/HyalS) spectrum was subtracted from the spectrum of the corresponding system containing the Fbg to obtain the difference spectrum of the protein, which reflects the secondary structure of the protein upon its interaction with the polymer. Protein characterization was derived from the comparison of the difference spectrum of interacting and native Fbg.

Fourier Self-Deconvolution (FSD) and Curve Fitting (CF) Analysis. Fourier self-deconvolution resolution enhancement was applied to narrow the widths of infrared bands and increase the separation of the overlapping components.

The self-deconvolution parameters were set according to Byler and Susi:[15] 14 cm^{-1} for the full bandwidth at half-height (fwhh) and 2.4 for the resolution enhancement factor. These values lend themselves to satisfactory resolution enhancement, enabling the determination of the number and position of the amide I component bands. The self-deconvolution method was used only to extract the essential input parameters for the curve fitting analysis that has been performed on the original amide I band spectrum.[17]

Before curve fitting was carried out, a two-point baseline correction at 1700/1600 cm^{-1} for the amide I band was performed, which allowed for a horizontal baseline. The curve fitting was accomplished employing Grams/AI software. The general procedure was as follows:

The components detected by the self-deconvolution method have been considered and entered into the program along with their respective positions and half-heights. The frequencies were fixed at the values previously determined by FSD, whereas the peak intensities were adjusted manually to obtain a fitting curve that could be superimposed with the original contour as far as possible.

All intensities were iterated to obtain the minimum rms (root-mean-square) error of differences between the original protein spectrum and the sum of all individual resolved bands.

All of the intensities and frequencies were fixed at the obtained values, while all of the widths were iterated.

All frequencies were iterated, and the other variables were kept constant.

After the iterative process was completed, the band areas of the peaks from 1700 to 1600 cm^{-1} were determined and expressed as a percentage of the total peak area in this range.

Only converged solutions with minimum values of reduced X^2 and standard deviations have been considered satisfactory.

As emphasized by Surewicz and Mantsch,[28] with these methods band narrowing is achieved at the expense of the original spectral shape. Consequently, despite its simplicity and potentiality, this type of data processing is not a routine procedure. On the contrary, the difficulties associated with obtaining artifact introduce a certain degree of subjectivity in the analysis and make the FSD method an analytical tool to use carefully, applying well-established data processing parameters.[47]

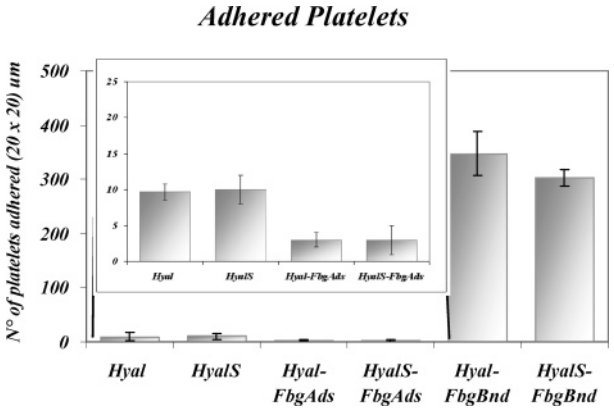

Figure 3. Platelets adhered on the tested surfaces.

Results

In Figure 2a is reported a schematic representation of two different approaches to functionalize the polysaccharide surfaces with adsorbed fibrinogen (A) or bound fibrinogen (B).

Each step of analysis was monitored by ATR FTIR spectroscopy, which demonstrated the complete covering of the coverslips by the polysaccharide and then of the polysaccharide layers by the Fbg.

Biological Analysis. *Platelet Adhesion and Activation.* The four samples were incubated with platelets suspended in PRP. In Figure 3 is reported the number of the platelets that adhered to the different materials when in PRP. Only a few platelets adhered on Hyal and HyalS surfaces. In this case, they showed limited shape deformation and can be classified as dendritic (disc-shaped morphology, few pseudopodia, and absence of spreading) and spread-dendritic (with several pseudopodia, some of them flattened onto the material surface and with hyaloplasm expanded among pseudopodia).

When Fbg was merely adsorbed on Hyal or HyalS, the number of adhered platelets decreased considerably and assumed a round shape characterized by the absence of pseudopodia. Furthermore, as is evident from the quantification of the PF4 release (Figure 4), these platelets had a low degree of activation,

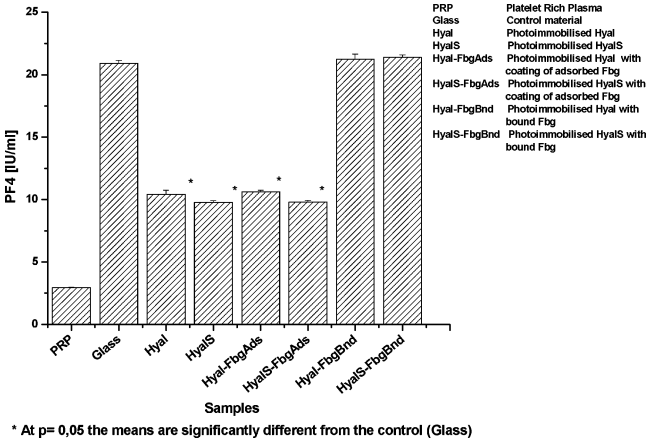

Figure 4. Activation of platelets as PF4 (IU/mL) in PRP after 3 h of incubation at 37 °C in static conditions. The amount of PF4 released from activated platelets was determined by ELISA assay.

much lower than that of the glass control material, but similar to that of the native Hyal and HyalS surfaces.

In contrast, Fbg_{Bnd} to Hyal and HyalS determined the formation of a platelet-carpet that completely covered the surface of the polysaccharide (Figure 5).

Platelets showed a fully spread morphology on glass as well and a high degree of activation: the amounts of PF4 released are the greatest of the series and comparable to that of the glass control material (Figure 4).

Table 3. Platelet Adhesion on Hyal and HyalS with and without Adsorbed or Bound Fibrinogen

sample	platelet behavior
Hyal	few dendritic (D) and/or spread-dendritic (SD)
HyalS	few dendritic (D) and/or spread-dendritic (SD)
Hyal-Fbg (Ads)	few round (R)
HyalS-Fbg (Ads)	few round (R)
HyalS-Fbg (bound)	fully spread (FS)
Hyal-Fbg (bound)	fully spread (FS)

The classification of platelet morphology after the interaction with the polysaccharide surfaces was summarized in Table 3.

Evaluation of the Role of Serum Proteins. The serum proteins present in the medium used for culturing platelets may potentially adsorb on the Fbg layer, interfering with the direct platelet−Fbg interaction.

Therefore, an SDS-PAGE analysis was carried out to ascertain the presence of proteins in the fractions eluted from the surfaces containing Fbg preincubated with serum proteins.

In the fractions eluted from all of the Hyal(S)-Fbg surfaces (either bound or adsorbed) pretreated with serum, proteins were detected only in the I and II H_2O fractions. As is evident in comparing Figure 6a and b, the first two H_2O fractions had electrophoretic profiles similar to that of serum. On the contrary, no proteins were detected in the other eluted fractions (Figure 6c−e), which demonstrated that serum proteins were not present on the surfaces containing Fbg.

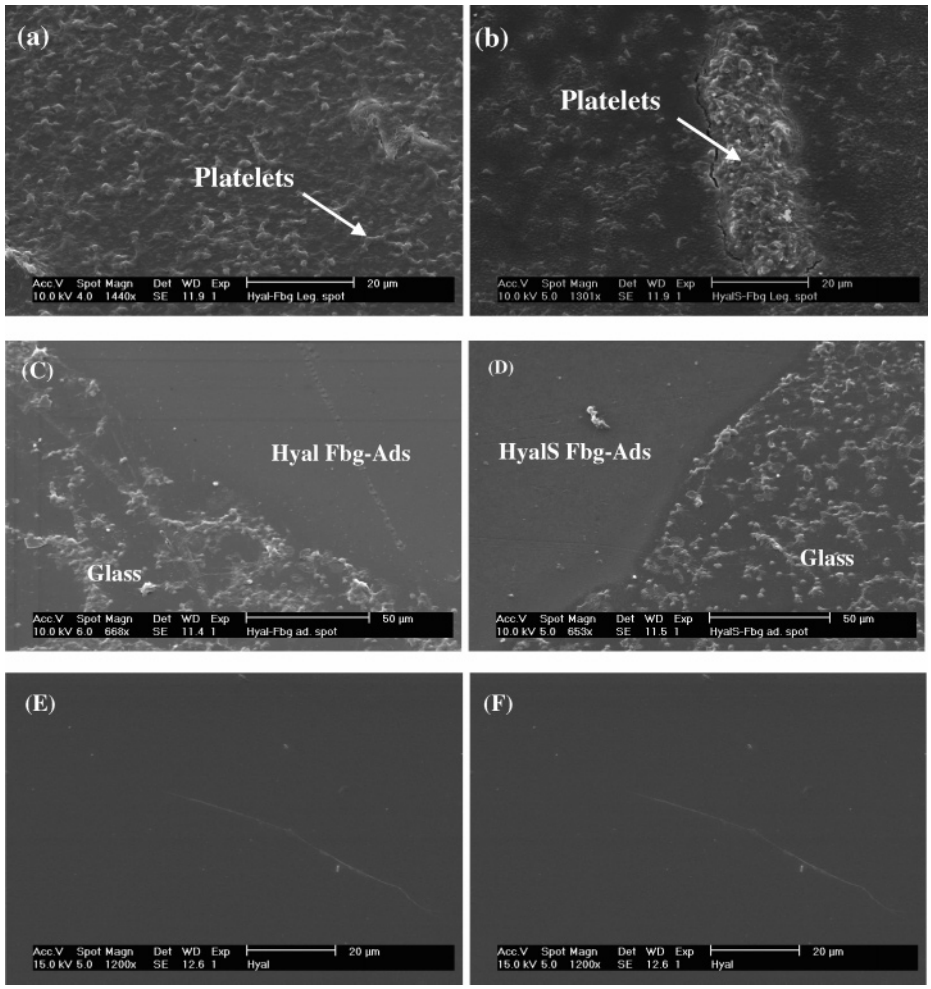

Figure 5. SEM images of platelets adhesion on Hyal-Fbg_{Bnd} (a) and HyalS-Fbg_{Bnd} (b); Hyal-Fbg_{Bnd} (c) and HyalS-Fbg_{Bnd} (d); and Hyal-Fbg_{Bnd} (e) and HyalS-Fbg_{Bnd} (f).

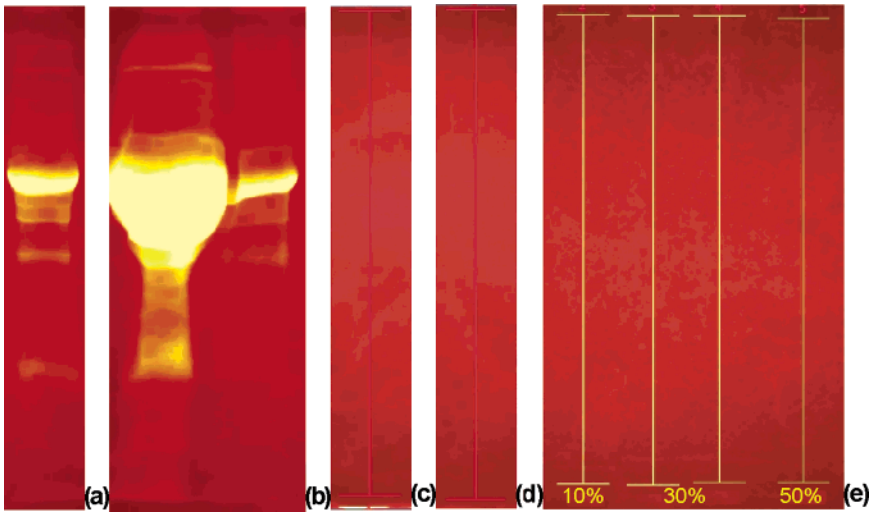

Figure 6. Electrophoretic patterns of fractions eluted from HyalS surfaces containing Fbg_{Bnd}: (a) serum; (b) I and II water fractions; (c) I Laemmli buffer fraction; (d) I modified Laemmli buffer fraction; and (e) isopropanol/water solution fractions.

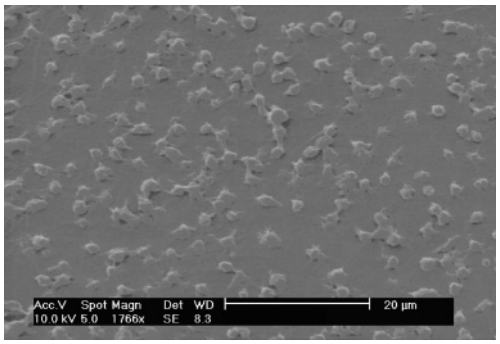

Figure 7. SEM image of platelet adhesion on glass after blocking the GPIIb/IIIa receptors.

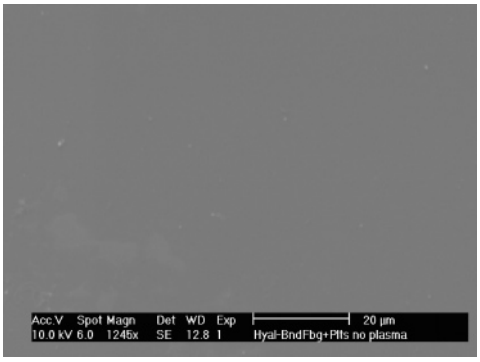

Figure 8. SEM image of platelet adhesion on Hyal(S)-Fbg_{Ads} and Hyal(S)-Fbg_{Bnd} surfaces after blocking the GPIIb/IIIa platelet membrane receptors.

The presence of Fbg evidently prevents the adsorption of further serum proteins, and consequently the only hypothesis that may be advanced is of weak and transient interfacial interactions among the surfaces and the soluble serum proteins.

To assess the molecular pathway involved in the surfaces containing Hyal(S)-Fbg platelets, the selective blocking of the GPIIb/IIIa platelet membrane receptors was performed. Only the control material (glass) was still able to induce platelet adhesion (see Figure 7), whereas no platelet adhesion occurred on all of the surfaces containing either adsorbed or bound Fbg (Figure 8).

On glass, the platelet adhesion even after the blocking of the GPIIb/IIIa may be due to the presence of other adhesive proteins

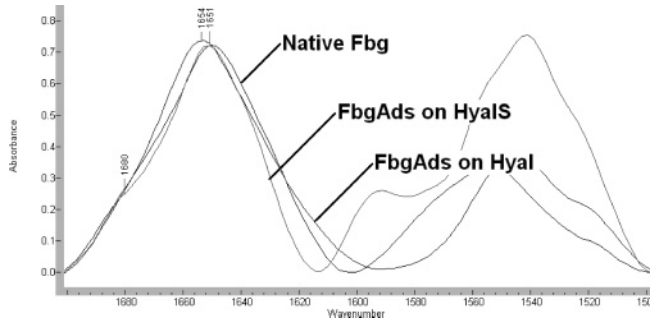

Figure 9. ATR-FTIR spectrum Fbg_{Ads} on Hyal, Fbg_{Ads} on HyalS, and native Fgb.

such as fibronectin, vitronectin, etc., which modulate platelet adhesion and activation.

Instead, on the Hyal(S)-Fbg_{Ads} and Hyal(S)-Fbg_{Bnd} surfaces, where no other proteins are adsorbed, the interaction between Fbg RIBS and GPIIb/IIIa LIBS is the only mechanism ruling the platelet adhesion.

Instrumental Analysis: Evaluation of Fbg Conformation. *ATR FT-IR, Fourier Self-Deconvolution (FSD), and Curve Fitting (CF) Analysis.* The conformational changes that occurred after Fbg adsorption or chemical binding on Hyal and HyalS surfaces were evaluated performing an ATR FTIR analysis combined with Fourier self-deconvolution and curve fitting calculations.

At first, the Fourier self-deconvolution was used to determine the number and the position of the amide I component bands. Next, the curve fitting analysis was done on the original amide I spectrum of each sample (Figures 9 and 10).

Details about the frequencies and the percentages of Fbg amide I composition are reported in Table 4.

As it can be seen in Figure 11, the native Fbg conformation consists of different coexisting structures: β-sheet (32%), α-helix (45%), and β-turns and bends (23%).[48,49]

When Fbg was adsorbed on Hyal, a strong rearrangement occurred (Figure 12).

A strong decrease of α-helix domains (from 45% to 22%) corresponded to an increase of the β-sheet component (from 32% to 52%), while the percentage of β-turns and bends did not change.

Fbg adsorption on HyalS surfaces, instead, determined a massive conversion of the α-helix domains (from 45% to 27%) mainly into new β-sheet structures.

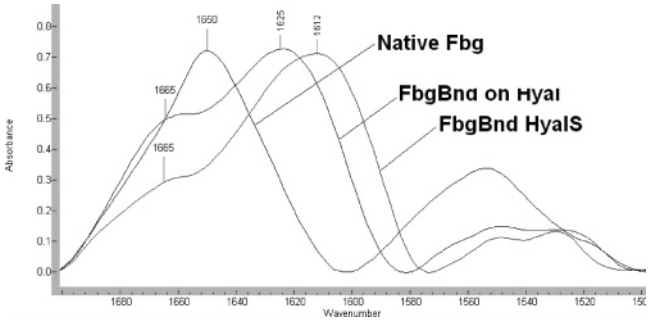

Figure 10. ATR-FTIR spectrum Fbg_{Bnd} on Hyal, Fbg_{Bnd} on HyalS, and native Fbg.

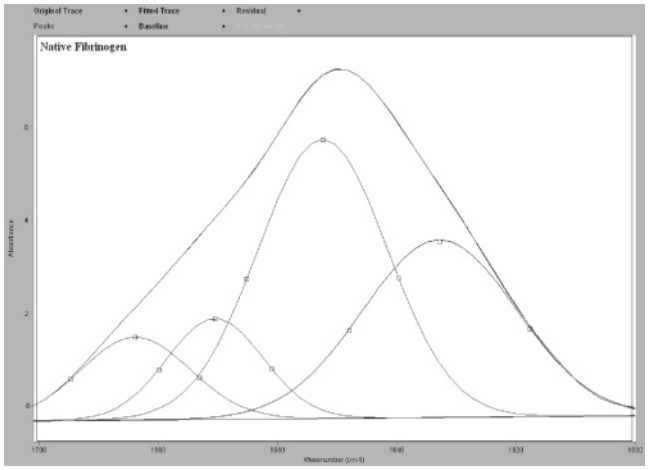

Figure 11. Native Fbg: amide I curve fitting.

According to Fabian et al.,[50] the shift of the amide I bands to a lower wavelength than those of the native protein is consequent to the protein interaction with the material. Therefore, the appearance of a band at 1625 cm^{-1} (Figure 13) demonstrated that a small percentage (11%) of β-sheet component Fbg interacted with the polysaccharide superficial chains by means of H-bonds and/or van der Wals forces.

The chemical immobilization of Fbg on the Hyal surfaces led to the complete disappearance of the α-helix component, the slight decrease of the β-turns and bends, and, overall, the massive formation (37%) of new low frequency antiparallel β-sheet structures (band at 1624 cm^{-1}) involved in stronger H-bonds and/or superficial van der Wals interactions with the polysaccharide surfaces (Figure 14).

Differently, the Fbg binding to HyalS surfaces determined a slight increment of the α-helix component (from 45% to 52%) and a simultaneous decrease of the β-turns and bands structures

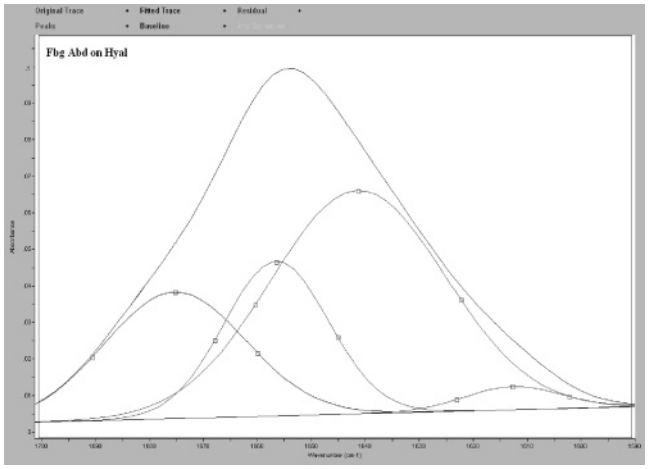

Figure 12. Fbg_{Ads} on Hyal: amide I curve fitting.

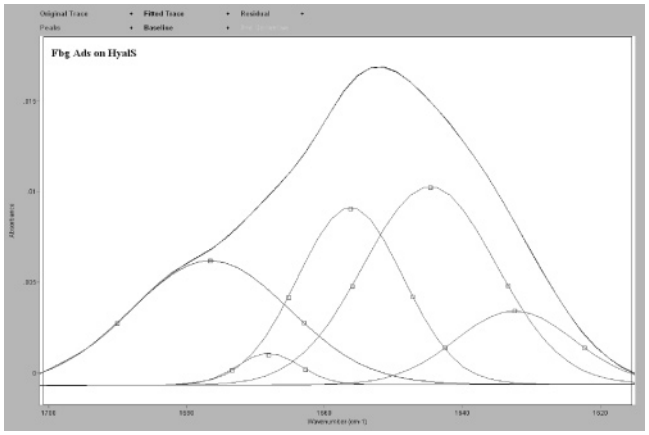

Figure 13. Fbg_{Ads} on HyalS: amide I curve fitting.

(Figure 15). In this case, the β-structures were represented only by one component band at 1619 cm^{-1} (36%). The shift to such low wavelengths with respect to the native Fbg β-structures can be interpreted as an evidence of the distortion of the β-type structures due to massive interaction with the polysaccharide chains.[50]

Discussion

Platelet adhesion and activation are important parameters characterizing the hemeocompatibility of biomaterials.[51,52] It is well known that the pre-adsorption of proteins on the material-surface, either as a multicomponent protein mixture or as a single

Table 4. Amide I Frequencies and Assignments

	extended chains							
	β-sheet							
	low components		high components		α-helix	unordered	turns and bends	
native Fbg			1634		1651		1670	1686
			(32%)		(45%)		(12%)	(11%)
Fbg Ads on Hyal	1612		1637		1656		1676	
	(3%)		(52%)		(22%)		(23%)	
Fbg Ads on HyalS		1628	1638		1652	1668		1681
		(11%)	(35%)		(27%)	(5%)		(22%)
Fbg Bnd on Hyal		1624	1638			1663		1689
		(37%)	(41%)			(13%)		(9%)
Fbg Bnd on HyalS	1619				1652		1674	
	(36%)				(52%)		(12%)	

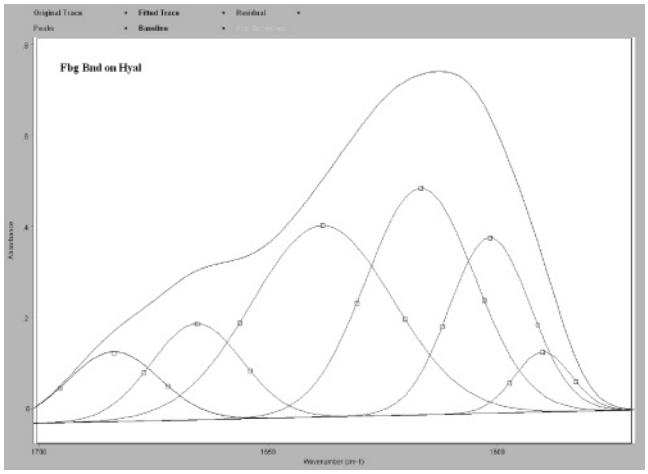

Figure 14. Fbg_{Bnd} on Hyal: amide I curve fitting.

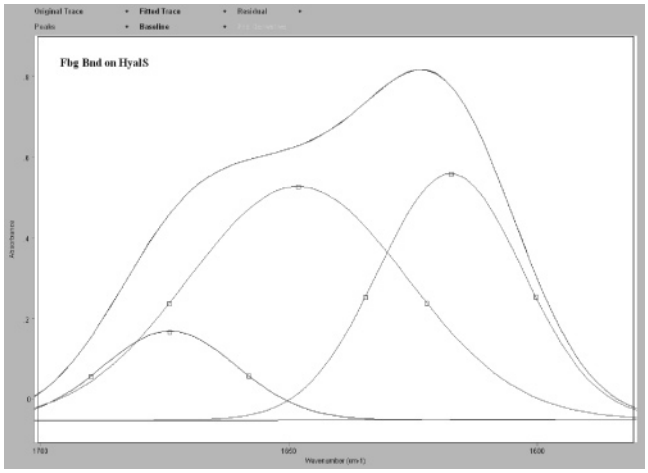

Figure 15. Fbg_{Bnd} on HyalS: amide I curve fitting.

protein solution, can improve or inhibit the adhesion and the activation of platelets.[53,54]

The ability to modulate the platelet response is related to several factors such as surface hydrophilicity and charge or protein mobility and orientation on the surface.

In an our previous work,[5] the adsorption or the chemical binding of fibronectin to the Hyal and HyalS surfaces enhanced the in vitro adhesion of the human fibroblasts on the polysaccharide surfaces.

Concerning the platelet adhesion and activation, several studies demonstrate the importance of Fbg distribution on the surface, emphasizing the necessity of considering not only the quantity of Fbg present on the surface but also the exposition of the peptide sequences regulating the interaction with the biological system.[55,56] Recently, Massa et al.[57] underlined the strict correlation existing between platelet adhesion, activation, and Fbg distribution and orientation that alter the manner by which platelets adhere to the surface.

Considering that the platelet−Fbg interaction is considered to be direct because no serum protein adsorption occurs either on the Fbg_{Ads} or on the Fbg_{Bnd} layer, our studies confirm this relationship and stress the importance of the protein conformation and orientation on the surface. In fact, despite the chemistry of the surface, the adsorption or the chemical binding of the Fbg to the polysaccharide led to considerable conformational changes that affect its "molecular potency". Moreover, as the interaction among the Fbg binding sequences and the GPIIb/IIIa LIBS (ligand-inducing binding site) is the only mechanism ruling platelet adhesion and activation, as demonstrated by the selective blocking of the GPIIb/IIIa platelet receptors, it is straightforward to affirm that the platelet adhesion and activation on the Hyal and HyalS surfaces containing Fbg is related to the rearrangement of the Fbg and precisely to the exposition of its receptor inducing binding sites (RIBS).

Actually, the conformational rearrangement of Fbg_{Ads} was different from that of the Fbg_{Bnd} and determined a different platelet response.

In the first case, after adsorption, the decrease of the α-helix components determined the formation of new β structures, of which just a small percentage interacted with the polysaccharide surfaces, completely unsetting the Fbg ability to express the adhesive activity.

In the latter case, the chemical immobilization of the polysaccharide chains led to a considerable distortion of the β-components of the Fbg, inducing the exposition of the Fbg RIBS and consequently platelet adhesion and activation.

Acknowledgment. We gratefully acknowledge the FIRB (Fondo per gli investimenti per la ricerca di base − MIUR) for financial support.

References and Notes

(1) Horbett, T. A. *Techniques for Proteins Adsorption Studies*; CRC: Boca Raton, FL, 1986; p 224.
(2) Curtis, A. S.; Forrester, J. V. *J. Cell Sci.* **1984**, *71*, 17−35.
(3) Andrade, J. *Surface and Interfacial Aspects of Biomaterial Polymers, Vol. 1: Surface Chemistry and Physics*; Plenum: New York, 1985; p 470.
(4) Lindon, M. J.; Minnett, T. W.; Tighe, B. J. *Biomaterials* **1985**, *6*, 396−402.
(5) Yamada, K. M.; Olden, K. *Nature* **1978**, *275*, 179−84.
(6) Grinnel, F.; Minter, D. *Proc. Natl. Acad. Sci. U.S.A.* **1978**, *75*, 4408−12.
(7) Barbucci, R.; Magnani, A.; Chiumiento, A.; Pasqui, D.; Cangioli, I.; Lamponi, S. *Biomacromolecules* **2005**, *6*, 638−645.
(8) Weissman, B.; Meyer, K. *J. Am. Chem. Soc.* **1954**, *76*, 1753.
(9) Band, P. A., Laurent, T. C., Eds. Portland Press: London, 1998; p 33.
(10) Fraser, J. R. E., Laurent, T. C., Comper, W. D., Eds. Harwood Academic Publishers: Amsterdam, 1996.
(11) Knudson, C. B.; Knudson, W. *FASEB J.* **1993**, 1233.
(12) Chen, W. Y.; Abatangelo, G. *Funct. Hyaluronan Wound Repair* **1999**, *2*, 79.
(13) Forrester, J.; Balazs, E. A. *Immunology* **1989**, *40*, 35.
(14) Akasuka, M.; Yamamoto, T.; Togetto, K.; Ando, T. *Agents Actions* **1993**, *38*, 122.
(15) Turner, N. J.; Cay, M. K.; Walzer, M. G.; Canfield, E. A. *Biomaterials* **2004**, *25*, 5995.
(16) Barbucci, R.; Magnani, A.; Leone, G. *Polymer* **2002**, *43*, 3541.
(17) Barbucci, R.; Benvenuti, M.; Casolaro, M.; Lamponi, S.; Magnani, A. *J. Mater. Sci.: Mater. Med.* **1994**, *5*, 830.
(18) Mourao, P. A.; Giumares, B.; Mulloy, B.; Gray, E. *J. Haematol.* **1998**, *101*, 647.
(19) Magnani, A.; Albanese, A.; Lamponi, S.; Barbucci, R. *Thromb. Res.* **1996**, *81*, 383.
(20) *Integrated Biomaterials Science*; Barbucci, R., Ed.; Kluwer Academic/Plenum Publishers: New York, 2002.
(21) Sen Gupta, A.; Wang, S.; Link, E.; Anderson, E. H.; Hofmann, C.; Lewandowski, J.; Kottke-Marchant, K.; Marchant, R. E. *Biomaterials* **2006**, *27*, 3084.
(22) Hongyan, B.; Zhong, W.; Meng, S.; Kong, J.; Yang, P.; Baohong, L. *Anal. Chem.* **2006**, *78*, 3399.
(23) Xu, H.; Kaar, J. L.; Russell, A. J.; Wagner, W. R. *Biomaterials* **2006**, *27*, 3125.
(24) Yu, S. H.; Mi, F. L.; Shyu, S. S.; Tsai, C. H.; Peng, C. K.; Lai, J. Y. *J. Membr. Sci.* **2006**, *276*, 68.
(25) Tsai, W. B.; Grunkemeier, J. M.; McFarland, C. D.; Horbett, T. A. *J. Biomed. Mater. Res.* **2002**, *60*, 348.
(26) Tsai, W. B.; Shi, Q.; Grunkemeier, J. M.; McFarland, C.; Horbett, T. A. *J. Biomater. Sci., Polym. Med.* **2004**, *15*, 817.
(27) Chinn, J. A.; Posso, S. E.; Horbett, T. A.; Ratner, B. D. *J. Biomed. Mater. Res.* **1991**, *25*, 535.

(28) Horbett, T. A. *BMES Bull.* **1999**, *23*, 5.
(29) Mosesson, M. W. *Fibrinogen Proteolysis* **2000**, *14*, 182−186.
(30) Standeven, K. F.; Ariëns, R. A.; Grant, P. J. *Blood Rev.* **2005**, *19*, 275−88.
(31) Bennett, J. S. *Ann. N.Y. Acad. Sci.* **2001**, *936*, 340−354.
(32) Rindi, G.; Manni, E. *Fisiol. Umana* **1998**, 1326.
(33) D'Souza, S. E.; Ginsberg, M. H.; Matsueda, G. R.; Plow, E. F. *Nature* **1991**, *350*, 66−68.
(34) Sims, P. J.; Ginsberg, M. H.; Plow, E. F.; Shattil, S. J. *J. Biol. Chem.* **1991**, *266*, 7345−7352.
(35) Shattil, S. J.; Hoxie, J. A.; Cunningham, M.; Brass, L. F. *J. Biol. Chem.* **1985**, *260*, 11107−11114.
(36) Zamarron, C.; Ginsberg, M. H.; Plow, E. F. *J. Biol. Chem.* **1991**, *266*, 16193−16199.
(37) Damme, H. S. V.; Feijen, J. In *Modern Aspects of Protein Adsorption on Biomaterials*; Missirlis, Y. F., Ed.; Kluver Academic: Lemm, 1991.
(38) Byler, D. M.; Susy, H. *Biopolymers* **1986**, *25*, 469.
(39) Magnani, A.; Lamponi, S.; Rappuoli, R.; Barbucci, R. *Polym. Int.* **1998**, *46*, 225−40.
(40) Barbucci, R.; Lamponi, S.; Magnani, A.; Pasqui, D. *Biomol. Eng.* **2002**, *19*, 161−70.
(41) Barbucci, R.; Magnani, A.; Lamponi, S.; Pasqui, D.; Bryan, S. *Biomaterials* **2003**, *24*, 915−926
(42) Barbucci, R.; Lamponi, S.; Aloisi, A. M. *Biomaterials* **2002**, *23*, 1967−197.
(43) Kot, M.; Lin, J. C.; Cooper, S. L. *Biomaterials* **1993**, *14*, 657−664.
(44) Rinella, J. R., Jr.; Workman, R. F.; Hermondson, M. A.; White, J. L.; Hem, S. L. *J. Colloid Interface Sci.* **1998**, *197*, 48.
(45) Laemmli, U. K. *Nature* **1970**, *277*, 680−685.
(46) Gottlien, M.; Chavko, M. *Anal. Biochem.* **1987**, *165*, 33.
(47) Surewicz, W. K.; Mantsch, H. H. *Biochim. Biophys. Acta* **1988**, *952*, 115.
(48) Chittur, K. K. *Biomaterials* **1998**, *19*, 357−69.
(49) Gendreau, R. M. Biomedical Fourier Transform Infrared Spectroscopy: Application to Proteins. In *Spectroscopy in the Biomedical Sciences*; Gendreau, R. M., Ed.; CRC Press: Boca Raton, FL, 1986; pp 21−52.
(50) Fabian, H.; Schultz, C.; Naumann, D.; Landt, O.; Hahn, U.; Saenger, W. *J. Mol. Biol.* **1993**, *232*, 967.
(51) Sefton, M. V.; Sawyer, A.; Gorbet, M.; Black, J. P.; Cheng, E.; Gemmell, C.; Pottinger-Cooper, E. *J. Biomed. Mater. Res.* **2001**, *14*, 263.
(52) Michanetzis, G. P. A.; Missirlis, Y. F. *J. Mater. Sci.: Mater. Med.* **1996**, *7*, 29.
(53) Brash, J. L. *J. Biomater. Sci., Polym. Ed.* **2000**, *11*, 1135.
(54) Grunkemeier, J. M.; Tsai, W. B.; Mcfarland, C. D.; Horbett, T. A. *Biomaterials* **2000**, *21*, 2243.
(55) Ikeda, M.; Ariyoshi, H.; Kambayashi, J. I.; Masato, S.; Kawasaki, T.; Monden, M. *J. Cell. Biochem.* **1996**, *61*, 292.
(56) Peerschke, E. I. B. *Am. J. Physiol.* **1995**, *259*, 611.
(57) Massa, T. M.; Yang, M. L.; Ho, J. Y. C.; Brash, J. L.; Santerre, J. P. *Biomaterials* **2005**, *26*, 7367.

BM060664M